

---

# EDDY COVARIANCE TOWERS AS SENTINELS OF ABNORMAL RADIOACTIVE MATERIAL RELEASES

---

THIS IS A DRAFT OF A MANUSCRIPT INTENDED FOR ENVIRONMENTAL SCIENCE AND POLLUTION RESEARCH  
DOI: 10.1000/XXXXX

 **Corresponding Author: Jemma Stachelek<sup>1</sup>**

<sup>1</sup> High Performance Computing Division  
Los Alamos National Laboratory  
Los Alamos, NM, USA, 87544  
jsta@lanl.gov

**Vachel A. Kraklow<sup>2</sup>**

<sup>2</sup> Earth and Environmental Sciences Division  
Los Alamos National Laboratory  
Los Alamos, NM, USA, 87544

**Elizabeth Christi Thompson<sup>3</sup>**

<sup>3</sup> Computer, Computational, and Statistical Sciences Division  
Los Alamos National Laboratory  
Los Alamos, NM, USA, 87544

**Lee Turin Dickman<sup>2</sup>**

<sup>2</sup> Earth and Environmental Sciences Division  
Los Alamos National Laboratory  
Los Alamos, NM, USA, 87544

**Emily Casleton<sup>3</sup>**

<sup>3</sup> Computer, Computational, and Statistical Sciences Division  
Los Alamos National Laboratory  
Los Alamos, NM, USA, 87544

**Sanna Sevanto<sup>2</sup>**

<sup>2</sup> Earth and Environmental Sciences Division  
Los Alamos National Laboratory  
Los Alamos, NM, USA, 87544

**Ann Junghans<sup>4</sup>**

<sup>4</sup> Nuclear and Engineering Nonproliferation Division  
Los Alamos National Laboratory  
Los Alamos, NM, USA, 87544

## **1 Abstract**

2 Ensuring accurate detection and attribution of abnormal releases of radioactive material is critical for protecting human  
3 health and safety. Most commonly, such detection is accomplished via active monitoring approaches involving the  
4 collection of physical samples. This is labor intensive and limits the temporal and spatial resolution of any detected  
5 events to a relatively coarse level. As an alternative first step towards passive monitoring, we developed an approach  
6 using eddy flux tower data records to identify signals from a known abnormal release and quantify the extent to which  
7 that signal also occurs at other times in the data record. Through two case-studies, one of which targeted the Fukushima  
8 nuclear disaster and the other targeting an abnormal release event at a radioisotope production facility in Fleurus  
9 Belgium, we tested our approach and identified several potential heretofore unidentified abnormal events that were  
10 consistent with atmospheric circulation patterns and/or wind direction from known release sites. Because our approach  
11 is relatively simple and is resistant to systematic errors in the observational record, it has broad applicability beyond  
12 specific constituents and ecosystem types to identify a wide variety of limited-duration anomalies in flux tower data to  
13 ensure human health and industrial safety.

14 **Keywords:** eddy covariance, data mining, industrial safety, vegetation response, radioactivity, photosynthesis

---

**15    1 Introduction**

16 Detecting abnormal releases of radioactive material (hereafter simply “abnormal releases”) is important as a means  
17 of ensuring human health and industrial safety. The detection of such releases is typically accomplished using active  
18 approaches that require site-specific sampling or trace gas measurements (Loyalka, 1983) sometimes as a part of  
19 international monitoring networks (e.g., Sangiorgi et al., 2020). A potential shortcoming of these active monitoring  
20 approaches is that they require collection of physical samples (particulates, gasses, and other signal carriers) to  
21 retrospectively determine the nature of the release and the events that may have led up to it. Active monitoring with  
22 such means is thus labor intensive and limits the temporal and spatial resolution of any detected events to a relatively  
23 coarse level.

24 A potential alternative to active monitoring is passive monitoring (e.g., the German Integrated Measuring and Information  
25 system and the International Monitoring System, Bieringer and Schlosser, 2004). Although existing wide area  
26 monitoring systems are already critical components of abnormal release detection and tracking programs (Medici, 2001),  
27 diversification-of-approach may increase the programs’ sensitivity and comprehensiveness. With a greater diversity  
28 of methods, monitoring programs may be able to detect a wider array of constituents with differing characteristics or  
29 expand their geographic extent without the need to deploy new instrumentation. In the present study, we developed a  
30 novel passive monitoring approach to supplement existing programs that involves the use of eddy covariance data to  
31 capture a signal from known abnormal releases. This signal is then used to investigate whether additional potential  
32 abnormal releases exist at other times in the data record. We focused on eddy flux towers, as they have the potential  
33 to provide abnormal release signatures, are globally distributed, have been in near continuous operation for several  
34 decades, and can be relatively cheaply and easily deployed in locations of interest. Therefore, they constitute a rich  
35 target for data mining approaches aimed at identifying signatures resulting from direct interference of radioactive  
36 material with target measurements and/or the indirect signal of vegetation responses to the deposition of radioactive  
37 material.

38 Our utilization of flux tower records for event discrimination stands in contrast to the typical use of data from the  
39 towers for direct carbon balance accounting. Whereas carbon balance accounting activities deal directly in the units of  
40 the measured data for computing quantities like net ecosystem exchange (Baldocchi et al., 2018), our use treats each  
41 variable as potentially including an indirect signal (i.e. an anomaly from normal vegetation behavior) of radioactive  
42 material deposition irrespective of its physical properties (e.g., mass, volume, etc). In this way, we are not directly  
43 measuring radioactive deposition but rather leveraging the fact that existing ecosystem monitoring records reflect  
44 vegetation photosynthesis rates and general stress condition of site vegetation in a known way (Nobel, 2020).

45 We specifically focused on short-term anomalies in the vegetation response data (on the order of days to weeks) due  
46 to either potential deposition of radioactive material or direct sensor effects rather than chronic long-term signals  
47 on the order of years to decades. In the first case study, we tested the ability of various data mining techniques to  
48 recover the signal from the closest tower (approximately 18 km away) to a known release coming from the Institut

des Radioelements (IRE) in Belgium nominally occurring on August 23, 2008. This release originated from waste tanks into the atmosphere and lasted for several days totaling 50 GBq  $^{131}I$ . The release went unreported (and possibly undetected) for several days. The first measurements in the vicinity of the facility were not taken until August 28th. These measurements found radioactivity levels of 5,000 Bq/kg in grass samples and led to a public health advisory for a 5km zone extending in a northeasterly direction from the facility (Carlé et al., 2010). Owing to the aforementioned measurement delays and the limited extent of the IRE release, we lack numeric estimates of the activity concentrations at tower locations. In the second case study, we further explored potential signals in flux tower data related to the Fukushima Nuclear Disaster occurring on March 11, 2011 releasing a massive radioactive plume that reached North America in 5 days that eventually dispersed throughout the entire northern hemisphere. An atmospheric dispersion study by Mészáros et al. (2016) estimates that our selected tower locations experienced deposition of particulate matter in the range of 0.44 - 31.08 mBq/m<sup>3</sup>.

We used the signal identified during the known release to identify additional potential abnormal releases occurring at other times in the data record and at other eddy flux towers. While the body of literature on direct or indirect effects of radioactive material on vegetation is limited, prior studies support the idea that exposure may cause declines in photosynthetic  $CO_2$  uptake. For example, Gudkov et al. (2019) detail how a wide range of exposure doses and durations can inhibit CO<sub>2</sub> uptake as a result of enzymatic effects on the Calvin Cycle. For the present study, we lack leaf-level observations to directly establish inhibition and instead express it as a change in the slope of the  $CO_2$  relationship with other environmental variables (e.g. air temperature, humidity, precipitation, etc.) before, during, and after exposure.

## 2 Methods

### 2.1 Data Description

For both the IRE and Fukushima case studiesy, we gathered measurements from eddy covariance platforms (i.e., “flux towers”) spanning multiple years. For the IRE case study, we targeted towers located in Belgium, which are part of the ICOS (Integrated Carbon Observation System) network available through the European Fluxes Database (<http://www.europe-fluxdata.eu/>). Three sites in proximity to the known release location had sufficient long-term data for our anticipated data mining efforts (BE-Lon, BE-Bra, and BE-Vie sites, Figure 1A). Each of the three flux tower sites are located within a crop ecosystem type and had almost 10 years of data available from 2004 through 2013 recorded at 30 min intervals. While BE-Lon had a near-continuous data record during this period, BE-Bra had a long period of missing data in 2005, and both BE-Bra and BE-Vie had a long period of missing data in 2009. The distance between IRE and the flux tower sites are approximately 19 km, 95 km, and 105 km for the BE-Lon, BE-Bra, and BE-Vie, respectively.

For the Fukushima case study, due to the direction of the plume, we gathered measurements from flux towers located in the Northern Hemisphere (Western United States), which are part of the Ameriflux network (<https://ameriflux.lbl.gov/>). To increase confidence that we are seeing a real effect, we contrasted the results from Northern Hemisphere sites, where

82 we expect a higher likelihood of impact, to measurements from flux towers located in the Southern Hemisphere, which  
83 are part of the OzFlux network (Cleverly, 2011). We selected sites with sufficient long-term data to cover the 2011 date  
84 of the disaster and excluded boreal sites with extreme snow cover related seasonality. We ultimately selected three sites  
85 (US-Wrc, US-GLE, and OZ-Mul, Figure 1B).

86 **2.2 Statistical Approach**

87 We processed each data file by 1) excluding nighttime measurements based on photosynthetic photon flux density  
88 (PPFD > 100  $\mu\text{mol m}^{-2} \text{s}^{-1}$ ) or net solar radiation (netrad > 0  $\text{W/m}^2$ ) and 2) defining an “event period” following  
89 the publicly released date of the abnormal release. We focused on the following variables as potentially containing a  
90 signature of the release : carbon dioxide, carbon dioxide flux (fc), latent heat (le), and sensible heat flux (h). Conversely,  
91 the following were treated as independent explanatory variables: wind speed, precipitation, atmospheric pressure,  
92 relative humidity, photosynthetic photon flux density, air temperature, and net radiation. Additionally, we used wind  
93 direction data from the eddy flux towers to determine when or if any released material might plausibly reach a particular  
94 location. All of the aforementioned data for each of these variables obtained from flux tower instrumentation recorded  
95 at a 30 minute (min) interval barring any gaps due to missing data.

96 To begin our analysis, we screened all pairwise, linear relationships between the aforementioned independent and  
97 dependent variables using a linear regression fit between each pair for the entire period of record (n=51). Variable  
98 pairs were excluded from further analysis if the overall coefficient of determination ( $R^2$ ) was less than 0.1. This low  
99 threshold was chosen to maximize the number of pairs that could potentially be investigated more deeply. From visual  
100 inspection, we determined that many of the rejected variable pairs appeared to have a nonlinear relationship. As our  
101 aim was to develop a methodology that could be applied broadly to other sites, we did not apply transformation to  
102 linearize these relationships without a physical justification for the transformation. Evaluating an exhaustive list of data  
103 transformations was beyond the scope of the present effort. After identification of candidate variable pairs, we fit an  
104 interaction model of the following form where Y represents a continuous response (e.g.,  $\text{CO}_2$ , latent heat, etc.),  $X_1$  is  
105 an independent variable (e.g., air temperature, humidity, etc.),  $W_2$  is a categorical variable representing the “period”  
106 of observation (i.e., during, before, or after, the event),  $\beta_0$  is the intercept,  $\beta_{1,2}$  are slope parameters for  $X_1$  and  $W_2$   
107 respectively, and  $\beta_3$  is the slope parameter for the interaction between  $X_1$  and  $W_2$ :

$$Y = \beta_0 + \beta_1 X_1 + \beta_2 W_2 + \beta_3 X_1 W_2$$

108 This interaction model was fit for a window of time encompassing the known release event and for every other possible  
109 window in the period-of-record. The overall length of the window was treated as an adjustable hyperparameter since  
110 the length of time for an abnormal material release to reach the footprint of the flux tower may be event-dependent  
111 and/or unknown. In addition, the length of time for deposited material to induce a possible vegetation response (or at  
112 least a flux data anomaly) is an unknown quantity. Thus, in the default base case, we set the window length (n\_days)

as 7 days, but we ran hyperparameter experiments to determine the result of setting it to longer periods of 10 and 14 days. The window length affects the duration of time designated as before and after the event. The period of time designated as during the event was set as 2 days in all cases. We compared the effect size of the interaction term ( $\beta_3$ ) during the event-encompassing window against all other windows in a “rolling” analysis. Therefore, the overall analysis compares the interaction term of the window of the known event against a window centered on every other observation. Specific windows that had an effect size at least as large as that of the known event and with wind conditions defined as “towards” the flux tower were flagged as “event detections”.

In order to flag event detections, we defined several adjustable hyperparameters to account for uncertainty surrounding atmospheric transport and the timing of any possible responses to material deposition. The first hyperparameter we defined, *wind\_tolerance*, reflects the range around the bearing from the facility to the tower location which we count as towards the tower. In the base default case, we set *wind\_tolerance* to 10 degrees, but we explored setting it to smaller values down to 5 degrees and larger values up to 20 degrees. The second hyperparameter we defined, *event\_quantile\_effect*, handles the unknown travel time of any materials to be deposited via an abnormal release or what, if any, delays exist between deposition and vegetation response. Rather than simply selecting the maximum value of  $\beta_3$  during a given window or the value at the exact time of the event, the value of *event\_quantile\_effect* is set to correspond with a specific quantile of all  $\beta_3$  values during the event window. In the base default case, this was set at 0.9, but we explored values as low as 0.5. Taken together, here is the overall logic we used to flag an event detection: consider a scenario where the effect size value (corresponding to the *event\_quantile\_effect* of the distribution of effect sizes during the *n\_days* window length) during a known event is X at a tower which is Z bearing from the known release location. An event detection would be flagged during any period where the effect size is  $\geq X$  and the wind direction is  $Z \pm wind\_tolerance$ .

All statistical analyses in the present study were carried out using the statsmodels Python package (Seabold and Perktold, 2009). Our processing scripts are openly available at <https://doi.org/10.5281/zenodo.13845254>, and we refer readers to the original providers for data access.

### 3 Results

For the IRE case study, among all possible pairwise combinations of dependent and independent variables (n=51, Table S1), we found that only the  $CO_2$  versus air temperature comparison had any measure of predictability from the model ( $R^2 > 0.05$ ) and a strong event effect size (Table 1). Although other variable pairs such as sensible heat flux and net radiation had a stronger effect size for the BE-Lon site, they had a weak linear relationship across the other sites. When we focus on the period of the abnormal release event in particular rather than the overall period of record, we found that  $CO_2$  versus air temperature relationship at each of the three focal towers had similar  $R^2$  values and effect sizes (Table 1). Figure 2 provides a visual example of the effect size framing in our analysis. Note how the apparent interaction effect between time periods around the abnormal release event in Figure 2A (i.e., different slopes for before, during,

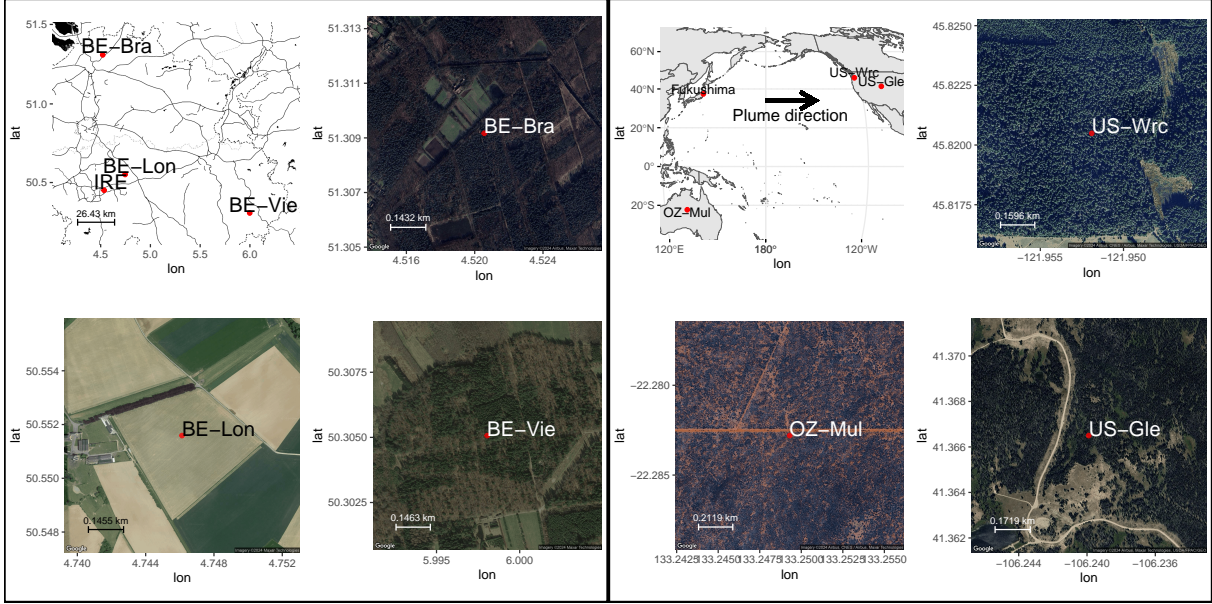


Figure 1: Map of flux tower locations for the IRE and Fukushima case studies (left and right respectively). Note that BE-Lon and BE-Vie are of a similar easterly direction to the IRE site whereas BE-Bra is in a northerly direction. The distance between IRE and the flux tower sites are approximately 19, 95, and 105 km for the BE-Lon, BE-Bra, and BE-Vie respectively. Each of the three IRE flux tower sites are located within a crop ecosystem type. Note that the US-Wrc site would be expected to have first contact with the Fukushima atmospheric plume followed by US-Gle. The OZ-Mul site would not be expected to have been affected by the plume.

146 after) translates to a relatively high effect size (Figure 2C) whereas in Figure 2B at an arbitrary time point, there is  
 147 no apparent interaction effect. This corresponds to a low effect size in Figure 2D. Note also how during and after the  
 148 known abnormal release, the slopes of the relationships between  $CO_2$  and air temperature become less negative than  
 149 before the event, with lower than expected  $CO_2$  at low air temperature (Figure 2A).

150 Despite the similar effect size at the three tower sites during the abnormal release event, they differed substantially in  
 151 the degree to which they uniquely flagged the known release event. At the BE-Lon and BE-Vie sites, our event detection  
 152 algorithm identified the known release and only a few other time periods as potential abnormal releases (Figure 3).  
 153 Conversely, at the northerly BE-Bra site, the algorithm was not able to identify the known release event distinct from  
 154 background noise. This can be seen in the rate of event detections ( $\alpha$ ) at each site, calculated as the number of event  
 155 detections divided by the total number of rolling windows in the period of record. This rate was less than 1% at the  
 156 BE-Lon and BE-Vie sites, but was greater than 2% at the BE-Bra site. It is notable that this ability to uniquely detect  
 157 the known release along with a plausible number of additional event detections corresponds with the fraction of the  
 158 abnormal release period when the wind was pointed from the release location towards the respective tower. The fraction  
 159 of the period of record where the wind was pointed from the facility toward the flux towers was much lower at the  
 160 BE-Bra site (5%) compared to the BE-Lon and BE-Vie sites (34% Table 1).

161 To increase our confidence that event detections were not dependent on the specific hyperparameters settings in our  
 162 base-case setup, we ran an exhaustive cross-validation set of hyperparameter experiments. For this effort, we tested every

Table 1: Overview of  $CO_2$  vs air temperature interaction models at the IRE site.  $R^2$  is the coefficient of determination of a linear model fit to the two covariates for the period of the abnormal release event (corresponding to “during” in Fig. 2). Effect is the event effect size of the interaction term ‘during’ the known release period matching the quantile of the distribution as specified by event quantile effect hyperparameter. Wind (%) is the average percentage of time that wind direction was from the site of known release towards the selected flux tower during the known release event. The remaining columns indicate the base-case hyperparameter settings.

Site	$R^2$	Effect	Wind(%)	Days(n)	Wind(tol)	Effect(q)
BE-Vie	0.35	36.2	34	7	10	0.9
BE-Bra	0.4	57.59	5	7	10	0.9
BE-Lon	0.47	30.13	34	7	10	0.9

163 possible combination of values for wind tolerance, number of days, and the event quantile effect. Across reasonable  
 164 values of specific hyperparameters, we found that their magnitudes had little effect on the rate at which events were  
 165 flagged as potential abnormal releases as even in the most extreme cases, we did not see detection rates exceeding  
 166 1%. We did, however, observe that the event detection was related to the window length and event quantile parameters  
 167 as shown by the slope of the line in Figure 4. Although increasing values of the event quantile parameter above the  
 168 limit of our tests ( $> 0.9$ ) would hypothetically increase event detection rates, we do not show this due to the noisiness  
 169 of the extreme quantiles of effect size distributions. Additionally, we do not show tests setting this parameter below  
 170 the median because it would lead to weak sensitivity to abnormal events. In a similar fashion as the event quantile  
 171 parameter, increasing the magnitude of the window length parameter would also likely increase the event detection rate  
 172 but here too we do not show tests setting this parameter beyond 14 days given the results of prior atmospheric modeling  
 173 efforts showing limited deposition at such long time scales (e.g. Mészáros et al., 2016).

174 For the Fukushima case study, our objective was to test the sensitivity of our approach to a broad scale abnormal release  
 175 and to introduce a control design to verify behavior on a flux tower where we expect no impact from any abnormal  
 176 releases. First, we verified that event detection specificity is present at towers likely to be exposed even across long  
 177 distances if the abnormal release is large (Figure 5). Then, we found a decrease in event detection specificity and an  
 178 increase in event detection rate moving from the flux tower expected to be most affected (US-Wrc), to a more distant  
 179 (likely less affected) tower (US-Gle), to a tower likely not exposed at all to the atmospheric plume (OZ-Mul, Figure 5).

## 180 4 Discussion

181 Using flux tower records collected closest to and in the prevailing wind direction to the IRE and the Fukushima release  
 182 locations, our event detection algorithm was able to identify both known abnormal releases and plausible previously  
 183 unidentified abnormal events. There was broad agreement among the closest flux tower and more distant flux towers  
 184 as to the timing and frequency of these releases, and our approach was supported by the loss of signal at flux towers  
 185 outside of the prevailing wind direction. This suggests that, at the very least, given a facility known to have a prior  
 186 abnormal release, flux tower networks are capable of providing a means of passive monitoring to detect subsequent  
 187 events as well as information on the environmental conditions before, during, and after the event. Furthermore, our

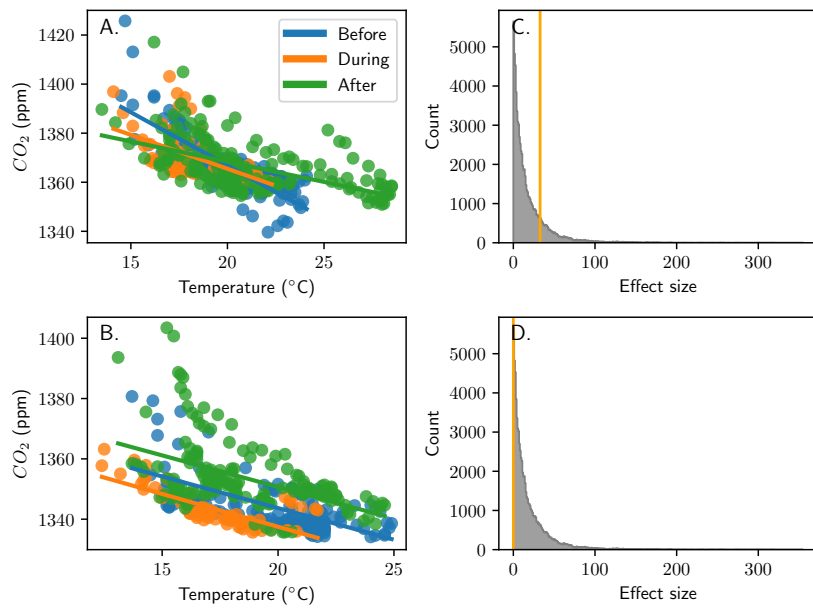


Figure 2: Interaction plots at the BE-Lon site between air temperature ( $C^{\circ}$ ) and  $CO_2$  (ppm) for the period of the known abnormal release (A) and an arbitrary non-release period (B). Also shown is the distribution of all interaction effect sizes (gray) compared with the effect size of the time period shown in the corresponding left panels (orange, C, D).

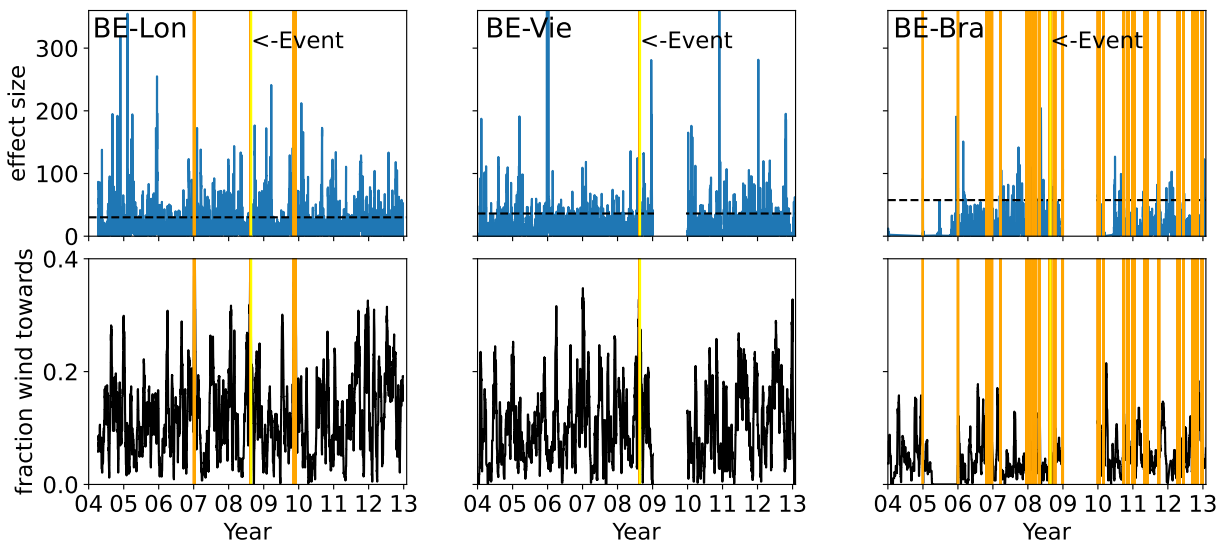


Figure 3: Time series plots (2004-2013) of rolling event detection analysis at the IRE site for the  $CO_2$  and air temperature ( $C^{\circ}$ ) variable pair. Event detection lines (orange), interaction effect size (blue), and event effect size (dashed black line) are shown in the top panels. The fraction of time that the wind direction was towards the particular tower (solid black) are shown in the corresponding bottom panels.

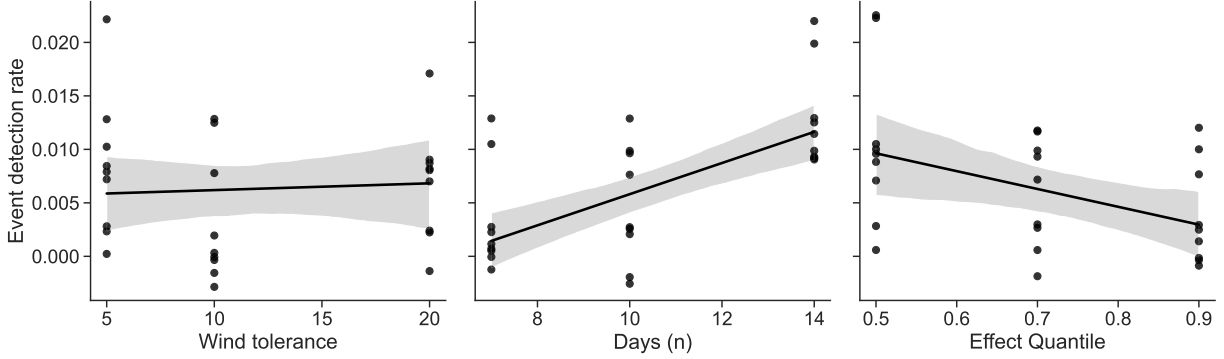


Figure 4: Sensitivity of event detection at the IRE site to different hyperparameter values (points) alongside potential relationship (solid line) and confidence interval (shaded region).

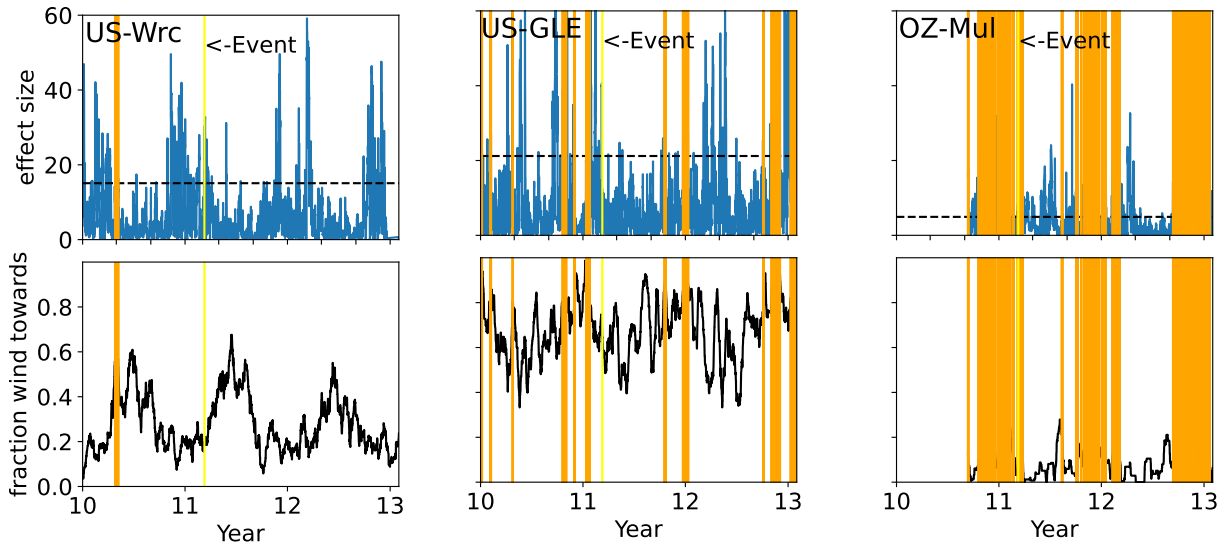


Figure 5: Time series plots (2010-2013) of rolling event detection analysis for the Fukushima disaster case study. The depicted variable pair is latent heat and relative humidity. Event detection lines (orange), interaction effect size (blue), and event effect size (dashed black line) are shown in the top panels. The fraction of time that the wind direction was towards the particular tower (solid black) are shown in the corresponding bottom panels.

188 approach has promise for situations when there is not a prior known abnormal release. In these cases, it may be possible  
 189 to continuously mine flux tower records (as they become available) for events that exceed some threshold identified in a  
 190 more comprehensive cross-site, cross-event benchmarking study. The delay between data collection and availability to  
 191 the general community via data repositories (e.g., Fluxnet) is highly variable among sites and investigators. In the best  
 192 case scenario, for actively monitored sites with responsive investigators, this can be as little as 6 months. As a result,  
 193 operationalization of our approach might target post-hoc attribution rather than real-time monitoring applications.  
 194 More generally, we show that flux tower records have value for this type of data mining despite the apparent noisiness  
 195 of the data (e.g., Fratini et al., 2018). We attribute the sensitivity of our approach to the fact that we fit successive  
 196 interaction models to limited sections of the data record, and we leveraged bivariate relationships to constrain noisiness  
 197 in individual data records. Our approach was aided by the fact that this type of scale-free data mining is largely  
 198 unaffected by systematic errors due to uncertainty in calibration standards and/or low resolution in specific sensor

199 packages deployed on the towers. This is because although such systematic errors may bias the magnitude of overall  
200 flux values, which would be a problem for typical uses of flux towers that deal directly in the units of the measured data,  
201 they do not reduce the overall confidence in individual values (Langford et al., 2015), which for our purposes might  
202 represent an abnormal release signal. The ability of our approach to identify a suitable release signature does likely  
203 depend on the quality and completeness of the underlying data.

204 Another contributor to the success of our approach was our ability to compare event detections at close towers in  
205 prevailing wind directions against more distant towers (refer to Figure 1), increasing our confidence that we were seeing  
206 a true signal and not spurious noise. The relatively dense networks of flux towers with long data records leveraged  
207 in both locations also aided these case studies. This level of flux tower density may be found in the United States,  
208 Western/Central Europe, Japan, and Australia, which have high densities of flux towers, but not throughout the rest  
209 of the world (Balocchi et al., 2001; Pastorello et al., 2020). As a result, this may impose geographical limits on  
210 our approach, although installation and maintenance of new flux towers in locations of interest may be cost effective  
211 compared to other monitoring approaches. Another attribute that likely aided our investigations was the fact that all  
212 three of the flux towers we examined were located in similar agricultural and forested ecosystem types for the IRE and  
213 Fukushima case studies respectively. Although investigating whether or not flux tower combinations with differing  
214 ecosystems would yield similar results is beyond the scope of the present study, we suspect that the data records among  
215 towers in disparate ecosystem types could differ too drastically to be of comparative use. For example, Pastorello et al.  
216 (2020) show that towers in the crop ecosystem type, of which all three sites used in this study belong, have a relatively  
217 narrow distribution of fluxes (i.e., gross primary production, GPP) compared to towers in the grassland or evergreen  
218 broadleaf forest types. One reason for this narrow spread in crop ecosystems may be the relative homogeneity of flux  
219 tower footprints in crop ecosystems, which typically extend to within 1000m of the tower depending on atmospheric  
220 conditions (e.g., wind speed and direction, Chu et al., 2021). Given that towers in other ecosystem types with a more  
221 heterogeneous flux tower footprint have a wider distribution of fluxes (e.g. Pastorello et al., 2020), we suspect that  
222 having all the towers in the IRE case study located in a homogenous ecosystem type was helpful in reducing the  
223 spikiness and spread of the data.

224 The biggest improvements to our approach would likely come from coupling our data mining procedure with rigorous  
225 air pollutant dispersion modeling (e.g., Mészáros et al., 2016). This would eliminate the need for indirect estimation  
226 of material transport via uncertainty analyses and instead use simulation results to analytically determine the likely  
227 arrival and duration of material deposition. Further improvements could be made by incorporating knowledge about  
228 the composition of materials being deposited (IAEA, 2006; Mészáros et al., 2016) and/or the interactions between  
229 material exposure and other environmental stressors (Mousseau and Møller, 2020), which likely affects the severity  
230 and timing of ecosystem responses and by extension the fluxes being measured by a given tower. Such information  
231 may help disentangle potential interference of atmospheric contaminants with infrared measurement of  $CO_2$  from  
232 declines in photosynthetic  $CO_2$  uptake of contaminated vegetation given our observation that during and after the  
233 known abnormal release, the slopes of the relationships between  $CO_2$  and air temperature become less negative than

before the event, with lower than expected  $CO_2$  at low air temperature. Although the chemical makeup of possible atmospheric contaminants is unknown, interference by iodine itself is unlikely to affect measurements of  $CO_2$  given that the absorption spectra of iodine peaks at much shorter wavelengths around 10-7 m (Haynes, 2016) compared to that of  $CO_2$  which peaks around 1700-2100 10-9 m (LICOR Biosciences Inc., Lincoln, NE).

The fact that we were able to identify known releases (along with potential unidentified abnormal events) in the data records from both a large event (i.e. Fukushima) as well as a smaller event despite not having a detailed radiological or atmospheric transport model is a strength of our approach. Furthermore, our approach is not limited to a radiological context, any abnormal event that affects the plant community and is reflected in flux tower data is a potential target. Because our approach is light-weight and resistant to systematic errors in the observational record, it has broad applicability beyond specific constituents and ecosystem types to identify a wide variety of limited-duration impacts to the plant community within flux tower footprints to ensure human health and industrial safety.

## References

- Baldocchi, D., Falge, E., Gu, L., Olson, R., Hollinger, D., Running, S., Anthoni, P., Bernhofer, C., Davis, K., Evans, R., et al., 2001. FLUXNET: A new tool to study the temporal and spatial variability of ecosystem-scale carbon dioxide, water vapor, and energy flux densities. *Bulletin of the American Meteorological Society*, 82(11):2415–2434.
- Baldocchi, D., Chu, H., and Reichstein, M., 2018. Inter-annual variability of net and gross ecosystem carbon fluxes: A review. *Agricultural and Forest Meteorology*, 249:520–533. doi:10.1016/j.agrformet.2017.05.015.
- Bieringer, J. and Schlosser, C., 2004. Monitoring ground-level air for trace analysis: Methods and results. *Analytical and Bioanalytical Chemistry*, 379(2):234–241. doi:10.1007/s00216-004-2499-z.
- Carlé, B., Perko, T., Turcanu, C., and Schröder, J., 2010. Individual response to communication about the August 2008  $^{131}I$  release in Fleurus: Results from a large scale survey with the Belgian population. *Session 19: Radiation and the society*, page 2774.
- Chu, H., Luo, X., Ouyang, Z., Chan, W. S., Dengel, S., Biraud, S. C., Torn, M. S., Metzger, S., Kumar, J., Arain, M. A., Arkebauer, T. J., Baldocchi, D., Bernacchi, C., Billesbach, D., Black, T. A., Blanken, P. D., Bohrer, G., Bracho, R., Brown, S., Brunsell, N. A., Chen, J., Chen, X., Clark, K., Desai, A. R., Duman, T., Durden, D., Fares, S., Forbrich, I., Gamon, J. A., Gough, C. M., Griffis, T., Helbig, M., Hollinger, D., Humphreys, E., Ikawa, H., Iwata, H., Ju, Y., Knowles, J. F., Knox, S. H., Kobayashi, H., Kolb, T., Law, B., Lee, X., Litvak, M., Liu, H., Munger, J. W., Noormets, A., Novick, K., Oberbauer, S. F., Oechel, W., Oikawa, P., Papuga, S. A., Pendall, E., Prajapati, P., Prueger, J., Quinton, W. L., Richardson, A. D., Russell, E. S., Scott, R. L., Starr, G., Staebler, R., Stoy, P. C., Stuart-Haëntjens, E., Sonnentag, O., Sullivan, R. C., Suyker, A., Ueyama, M., Vargas, R., Wood, J. D., and Zona, D., 2021. Representativeness of Eddy-Covariance flux footprints for areas surrounding AmeriFlux sites. *Agricultural and Forest Meteorology*, 301–302:108350. doi:10.1016/j.agrformet.2021.108350.

- 266 Cleverly, J., 2011. Alice springs mulga OzFlux site. *OzFlux: Australian and New Zealand flux research and monitoring*  
267 *network, hdl*, 102(100):8697.
- 268 Fratini, G., Sabbatini, S., Ediger, K., Riensche, B., Burba, G., Nicolini, G., Vitale, D., and Papale, D., 2018. Eddy  
269 covariance flux errors due to random and systematic timing errors during data acquisition. *Biogeosciences*, 15(17):  
270 5473–5487. doi:10.5194/bg-15-5473-2018.
- 271 Gudkov, S. V., Grinberg, M. A., Sukhov, V., and Vodeneev, V., 2019. Effect of ionizing radiation on physiological and  
272 molecular processes in plants. *Journal of Environmental Radioactivity*, 202:8–24. doi:10.1016/j.jenvrad.2019.02.001.
- 273 Haynes, W. M., 2016. *CRC Handbook of Chemistry and Physics*. CRC press.
- 274 IAEA, 2006. *Radiological Conditions in the Dnieper River Basin*. Radiological Assessment Reports Series. International  
275 Atomic Energy Agency, Vienna. ISBN 92-0-104905-6.
- 276 Langford, B., Acton, W., Ammann, C., Valach, A., and Nemitz, E., 2015. Eddy-covariance data with low signal-to-noise  
277 ratio: Time-lag determination, uncertainties and limit of detection. *Atmospheric Measurement Techniques*, 8(10):  
278 4197–4213. doi:10.5194/amt-8-4197-2015.
- 279 Loyalka, S., 1983. Mechanics of aerosols in nuclear reactor safety: A review. *Progress in Nuclear Energy*, 12(1):1–56.  
280 doi:10.1016/0149-1970(83)90024-0.
- 281 Medici, F., 2001. The IMS radionuclide network of the CTBT. *Radiation Physics and Chemistry*, 61(3-6):689–690.  
282 doi:10.1016/S0969-806X(01)00375-9.
- 283 Mészáros, R., Leelőssy, Á., Kovács, T., and Lagzi, I., 2016. Predictability of the dispersion of Fukushima-derived  
284 radionuclides and their homogenization in the atmosphere. *Scientific Reports*, 6(1):19915. doi:10.1038/srep19915.
- 285 Mousseau, T. A. and Møller, A. P., 2020. Plants in the Light of Ionizing Radiation: What Have We Learned From  
286 Chernobyl, Fukushima, and Other “Hot” Places? *Frontiers in Plant Science*, 11:552. doi:10.3389/fpls.2020.00552.
- 287 Nobel, P., 2020. *Physicochemical and Environmental Plant Physiology*. Elsevier. ISBN 978-0-12-819146-0.  
288 doi:10.1016/C2018-0-04662-9.
- 289 Pastorello, G., Trotta, C., Canfora, E., Chu, H., Christianson, D., Cheah, Y.-W., Poindexter, C., Chen, J., Elbashandy, A.,  
290 Humphrey, M., et al., 2020. The FLUXNET2015 dataset and the ONEFlux processing pipeline for eddy covariance  
291 data. *Scientific data*, 7(1):225.
- 292 Sangiorgi, M., Hernández-Ceballos, M. A., Jackson, K., Cinelli, G., Bogucarskis, K., De Felice, L., Patrascu, A., and  
293 De Cort, M., 2020. The European Radiological Data Exchange Platform (EURDEP): 25 years of monitoring data  
294 exchange. *Earth System Science Data*, 12(1):109–118. doi:10.5194/essd-12-109-2020.

**295 Statements and Declarations****296 Funding**

297 We acknowledge funding for supporting the AmeriFlux data portal: U.S. Department of Energy Office of Science.  
298 The data used in this activity has been also funded by CarboEuropeIP (EU-FP6), IMECC (EU-FP6). This work was  
299 supported by Los Alamos National Laboratory (LDRD-20220062ER).

**300 Competing Interests**

301 The authors have no relevant financial or non-financial interests to disclose.

**302 Author Contributions**

303 JS built models, analyzed data, and wrote the paper. SS, LTD, and AJ contributed to the conception of the manuscript.  
304 ECT, VAK, LTD, and EC edited the manuscript. All authors provided interpretation of results.

**305 Ethical Approval**

306 Not applicable

**307 Consent to Participate**

308 Not applicable

**309 Consent to Publish**

310 Not applicable

**311 Availability of Data and Materials**

312 No new data was produced in this study. All original data used is available publicly from their respective sources and  
313 archived permanently with restrictions on redistribution. These can be found at <http://www.europe-fluxdata.eu/>,  
314 <https://fluxnet.org/>, and (Cleverly, 2011).

315 Computer code and secondary data reuse that supports the results and analyses of the paper are available at:  
316 <https://doi.org/10.5281/zenodo.13845254>.